Heteronuclear Recoupling in Solid-State Magic-Angle-Spinning NMR via Overtone Irradiation

Sungsool Wi and Lucio Frydman*

Contribution from the Department of Chemical Physics, Weizmann Institute of Sciences, 76100 Rehovot, Israel, and Department of Chemistry (M/C 111), University of Illinois at Chicago, 845 West Taylor Street, Chicago, Illinois 60607-7061

Received June 5, 2001. Revised Manuscript Received August 1, 2001

Abstract: A heteronuclear dipolar recoupling scheme applicable to $I-S$ spin pairs undergoing magic-angle-spinning (MAS) is introduced, based on the overtone irradiation of one of the coupled nuclei. It is shown that when I is a quadrupole, for instance ^{14}N, irradiating this spin at a multiple of its Larmor frequency prevents the formation of MAS dipolar echoes. The ensuing S-spin signal dephasing is significant and dependent on a number of parameters, including the $I-S$ dipolar coupling, the magnitude of I's quadrupolar coupling, and the relative orientations between these two coupling tensors. When applied to a spin-1 nucleus, this overtone recoupling method differs from hitherto proposed recoupling strategies in that it involves only the $|\pm 1\rangle$ I_z eigenstates. Its dephasing efficiency becomes independent of first-order quadrupolar effects yet shows a high sensitivity to second-order offsets. A constant-time/variable-offset recoupling sequence thus provides a simple route to acquire, in an indirect fashion, ^{14}N overtone spectra from rotating powders. The principles underlying this kind of S-^{14}N experiments and different applications involving $S = {}^{13}$C, ^{59}Co sites are presented.

1. Introduction

Dipole−dipole interactions between nuclear spins provide a valuable tool for probing molecular and macromolecular structures.[1−3] When NMR experiments are carried out in the solid phase, such couplings can be directly measured and used to extract internuclear distances. Complications arise, however, upon attempting to determine these couplings while executing magic-angle-spinning (MAS). Throughout each rotor period, this procedure will average away all couplings that transform as second rank tensors, including the dipolar couplings. A solution to this problem is offered by double-resonance techniques.[4−9] These protocols exploit the fact that dipolar Hamiltonians are given by products of spatial- and spin-dependent terms, to prevent the MAS averaging of the spatial couplings via synchronous radio frequency (rf)-driven motions of the spins. For instance, when heteronuclear $I-S$ pairs of spin-$^1/_2$ nuclei are involved, net dipolar evolutions can be imposed on an S signal by inverting the I_z eigenstates with rotor-synchronized π pulses (rotational-echo double-resonance, REDOR),[4−10] through continuous nutations of the I_z states at integer multiples of the sample spinning speed ω_r (rotary resonance recoupling, R^3),[11,12] or via the application of more complex forms of amplitude- and phase-modulated I rf fields.[13−15]

Although they are of widespread use in the spectroscopy of biological, organic, and inorganic materials, the applicability of these recoupling strategies gets compromised when quadrupolar $I \geq 1$ nuclei are involved. Challenges arise in these cases from the fact that the applied rf nutation fields have to compete with much larger internal coupling frequencies stemming from the quadrupole interaction. A typical example of these complications is furnished by ^{14}N, a 99.6% abundant $I = 1$ nucleus. These spins are often subject to megahertz-sized quadrupole effects which can overwhelm the nutation effects introduced by the rf irradiation. Most of the manipulations proposed for the recoupling of spin-$^1/_2$ become in these cases unachievable, or at best subject to a very different spin physics. As a result of this, quadrupole-specific recoupling strategies had to be developed for interfering with the dipolar MAS modulation.[16−20] One of the most widely applicable principles available for manipulating strongly coupled quadrupolar sites in a rotor-synchronized fashion is that relying on the transfer of populations via adiabatic

* To whom correspondence should be addressed at the Weizmann Institute of Science. Fax: +972-8-9344123. E-mail: lucio.frydman@weizmann.ac.il.

(1) Slichter, C. P. *Principles of Nuclear Magnetic Resonance*; Springer-Verlag: New York, 1990.
(2) Hahn, E. L. *Phys. Rev.* **1950**, *80*, 580.
(3) Kaplan, D. E.; Hahn, E. L. *J. Phys. Radium* **1958**, *19*, 821.
(4) Gullion, T.; Schaefer, J. *Adv. Magn. Reson.* **1989**, *13*, 57.
(5) Grifiths, J. M.; Griffin, R. G. *Anal. Chim. Acta* **1993**, *283*, 1081.
(6) Bennett, A. E.; Griffin, R. G.; Vega, S. In *NMR: Basic Principles and Progress*; Blumich, B., Kosfeld, R., Eds.; Springer-Verlag: Heidelberg, 1994; Vol. 33, p 3.
(7) Gullion, T. *Concepts Magn. Reson.* **1998**, *10*, 277.
(8) Dusold, S.; Sebald, A. *Annu. Rep. NMR Spectrosc.* **2000**, *41*, 185.
(9) Gullion, T.; Pennington, C. H. *Chem. Phys. Lett.* **1998**, *290*, 88.
(10) Gullion, T.; Schaefer, J. *J. Magn. Reson.* **1989**, *81*, 96.
(11) Levitt, M. H.; Oas, T. G.; Griffin, R. G. *Isr. J. Chem.* **1988**, *28*, 271.
(12) Oas, T. G.; Levitt, M. H.; Griffin, R. G. *J. Chem. Phys.* **1988**, *89*, 692.
(13) Fu, R. Q.; Smith, S. A.; Bodenhausen, G. *Chem. Phys. Lett.* **1997**, *272*, 361.
(14) Takeda, K.; Terao, T.; Takegoshi, K. *Chem. Phys. Lett.* **1996**, *260*, 331.
(15) Ishii, Y.; Terao, T. *J. Chem. Phys.* **1998**, *109*, 1366.
(16) Grey, C. P.; Veeman, W. S. *Chem. Phys. Lett.* **1992**, *192*, 379.
(17) Grey, C. P.; Veeman, W. S.; Vega, A. J. *J. Chem. Phys.* **1993**, *98*, 7711.
(18) Grey, C. P.; Vega, A. J. *J. Am. Chem. Soc.* **1995**, *117*, 8232.
(19) Gullion, T. *Chem. Phys. Lett.* **1995**, *246*, 325.
(20) Ba, Y.; Kao, H.-M.; Grey, C. P.; Chopin, L.; Gullion, T. *J. Magn. Reson.* **1998**, *133*, 104.

10.1021/ja0113798 CCC: $20.00
Published on Web 09/29/2001

passages.[21] In these experiments, which possess no close analogue in the spin-$^1/_2$ realm, changes in the I_z states are implemented by a continuous rf irradiation that solely becomes effective when MAS nullifies the much larger first-order quadrupolar effects. As for all crystallites this happens only a few times per rotor period, the result is an effective interference with the modulation imposed by MAS on the spatial terms of the dipolar coupling, and a net re-introduction of the latter. These are the principles underlying the continuous transfer of populations by double-resonance (TRAPDOR) recoupling strategy,[16−18] as well as the recoupling by adiabatic passage double-resonance (REAPDOR) technique.[19,20,22]

The present study explores an alternative for recoupling strongly coupled *I* quadrupoles under MAS, based on irradiating these nuclei at a multiple of their Larmor frequencies. For a spin-1 like ^{14}N, the main consequence of implementing such a recoupling is that it becomes independent of the first-order quadrupolar interaction. Indeed, overtone irradiation at twice the ω_0^I Larmor frequency excites solely the usually forbidden $|+1\rangle \leftrightarrow |-1\rangle$ transition, affected only by second-order quadrupole effects.[23−27] Although such transitions violate the usual high-field NMR selection rule, they become feasible when quadrupolar couplings χ_q are strong enough to substantially tilt the spins' axes of quantization. The nutation rates that are then imposed on the spins by overtone irradiation fields ω_1 are in the order of $\omega_1\chi_q/\omega_0^I$. For ^{14}N $\chi_q/\omega_0^I \approx 0.1$; consequently, conventional rf irradiation strengths will produce rotary nutations in the kilohertz range, capable of effectively interfering with MAS averaging at the usual spinning rates. As is further discussed below, the time dependence that MAS induces on the first-order quadrupole coupling also splits up the overtone nutation frequencies into a sideband spectrum spaced at multiples of ω_r, that further contributes to an efficient $I-S$ dipolar recoupling regardless of the strength of $|\chi_q|$. Throughout this study we shall refer to these phenomena as overtone rotary recoupling (ORR); the following sections introduce the basic features of these new experiments, discuss their complementary nature vis-à-vis currently available recoupling techniques, and demonstrate their potentially widespread applicability not only for measuring ^{14}N$-S$ dipolar couplings but also as simple means to acquire ^{14}N overtone spectra from rotating powders.

2. Principles of Overtone-Driven Recoupling

2.1. The Overtone Excitation. Although overtone recoupling could, in principle, be applied on a variety of strongly coupled quadrupolar species, we shall restrict this analysis to the simplest $I = 1$ case, using ^{14}N as an example. To describe the details of ^{14}N$-S$ overtone recoupling, it is necessary first to discuss the basic spin dynamics occurring during overtone irradiation. Therefore, although the focus of this work will eventually become a heteronuclear spin pair on which the *S*-spin signal is detected, we begin centered on an $I = 1$ spin subject to a sizable quadrupole interaction as well as to an overtone rf field. As discussed elsewhere, understanding overtone nutation requires starting from the laboratory-frame Hamiltonian,[23,26,28] which for such systems will be assumed given by

$$H_{lab} = H_Z^I + H_Q^I + H_{rf} \tag{1}$$

$H_Z^I = -\omega_0^I I_Z$ is *I*'s Zeeman interaction, and following the notation given in refs 26 and 28, quadrupole and rf interactions are written as

$$H_Q^I = \chi_Q[\sqrt{6}T_{2,0}a + T_{2,1}f - T_{2,-1}f^* + T_{2,2}g + T_{2,-2}g^*] \tag{2}$$

$$H_{rf} = 2\omega_1(I_x \sin\theta + I_z \cos\theta)\cos(\omega_{irr}t) \tag{3}$$

H_Q^I is here given in terms of products between the irreducible spin-space spherical components $\{T_{2,m}\}_{-2\le m\le 2}$, and the complex functions $\{a,f,g\}$ depending on the asymmetry parameter η_Q and on Euler angles relating quadrupolar and Zeeman principal axes systems (PASs). χ_Q represents the strength of the quadrupolar interaction, given in frequency units by the standard definition $\chi_Q = e^2qQ/[4I(2I-1)\hbar]$. H_{rf} in turn is defined by an amplitude ω_1, an angle of coil inclination θ with respect to B_0, and an oscillation frequency ω_{irr} in the neighborhood of $2\omega_0^I$. To reproduce overtone phenomena it is necessary to consider, at least to first order, the corrections that H_Q^I will impose on the high-field Zeeman eigenstates. For $I = 1$ this entails considering the tilting matrix[29]

$$T = \begin{bmatrix} 1 & -\dfrac{\epsilon f^*}{\sqrt{2}} & \dfrac{\epsilon g}{2} \\ \dfrac{\epsilon f^*}{\sqrt{2}} & 1 & \dfrac{\epsilon f}{\sqrt{2}} \\ -\dfrac{\epsilon g^*}{\sqrt{2}} & -\dfrac{\epsilon f^*}{\sqrt{2}} & 1 \end{bmatrix} \tag{4}$$

that diagonalizes a quadrupole-perturbed Zeeman interaction to first order in $\epsilon = \chi_Q/\omega_0^I$. The Hamiltonian in this tilted frame, $H_{tilt} = T^\dagger H_{lab} T$, is

$$H_{tilt} = \begin{bmatrix} \omega_q^{(1)} + \omega_q^{(2)} - \omega_0^I & 0 & \omega_1\epsilon(f\cos\theta + g\sin\theta) \\ 0 & -2\omega_q^{(1)} & 0 \\ \omega_1\epsilon(f^*\cos\theta + g^*\sin\theta) & 0 & \omega_q^{(1)} - \omega_q^{(2)} + \omega_0^I \end{bmatrix} \tag{5}$$

where $\omega_q^{(1)} = \chi_Q a$ is the usual definition for the first-order quadrupolar coupling, and $\omega_q^{(2)} = \chi_Q^2(|f|^2 + |g|^2)/\omega_0^I$ is the second-order quadrupolar coupling. Within this tilted-frame approximation, the overtone rf irradiation Hamiltonian will only connect $|\pm 1\rangle$ eigenstates, for which the first-order quadrupole coupling $\omega_q^{(1)}$ acts as a mere energy shift. This, together with the unperturbed state, $|0\rangle$, can thus be dropped altogether from the relevant Liouville space where spin evolution takes place. A usual rotating-frame transformation $R = \exp(i\omega_0^I I_z t)$ then leads to the effective spin-$^1/_2$ overtone nutation Hamiltonian[28]

$$H_{nutation} = (R^{-1}H_{tilt}R)_{|+1\rangle,|-1\rangle} = \begin{bmatrix} \Delta + \omega_q^{(2)} & \epsilon\omega_1(f\cos\theta + g\sin\theta) \\ \epsilon\omega_1(f^*\cos\theta + g^*\sin\theta) & -\Delta - \omega_q^{(2)} \end{bmatrix} \tag{6}$$

where for completion we have introduced the potential of

(21) Vega, A. J. *J. Magn. Reson.* **1992**, *96*, 50.
(22) Chopin, L.; Vega, S.; Gullion, T. *J. Am. Chem. Soc.* **1998**, *120*, 4406.
(23) Bloom, M.; LeGros, M. A. *Can. J. Phys.* **1986**, *64*, 1522.
(24) Tycko, R.; Opella, S. J. *J. Am. Chem. Soc.* **1986**, *108*, 3531.
(25) Tycko, R.; Stewart, P. L.; Opella, S. J. *J. Am. Chem. Soc.* **1986**, *108*, 5419.
(26) Tycko, R.; Opella, S. J. *J. Chem. Phys.* **1987**, *86*, 1761.
(27) Tycko, R. In *Encyclopedia of NMR*; Grant, D. M., Harris, R. K., Eds.; J. Wiley & Sons: Chichester, 1996; p 3425.
(28) Marinelli, L.; Wi, S.; Frydman, L. *J. Chem. Phys.* **1999**, *110*, 3100.
(29) Landau, L. D. *Quantum Mechanics*; Pergamon: Oxford, 1991.

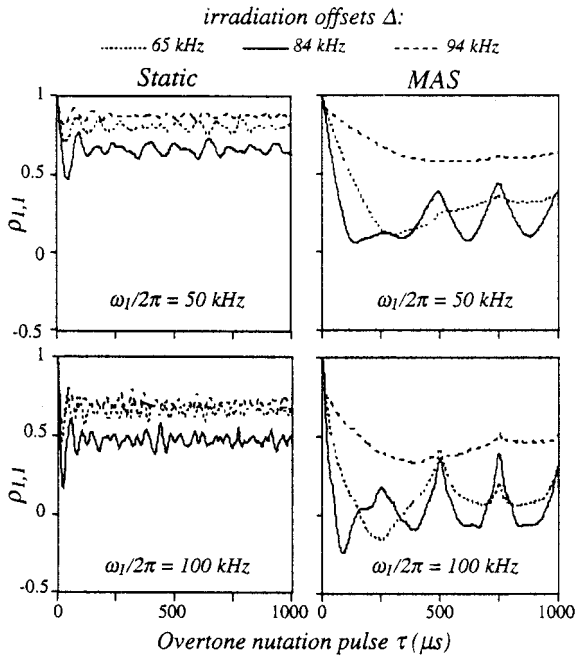

Figure 1. Comparisons between the overtone nutation of the $I_z = |+1\rangle$ quantum state ($\rho_{1,1}$ element of I's density matrix) under static and MAS conditions, as a function of the rf offset and pulse irradiation time τ. Curves were calculated for 50 and 100 kHz rf field strengths, $\chi_Q/2\pi =$ 0.8 MHz, $\eta_Q = 0.2$, spinning speed = 4 kHz, $2\omega_0^I/2\pi = 43.6$ MHz, 20^3 powder-averaged orientations. For the numerical MAS propagations a $\Delta\tau \approx 1.95$ μs time increment was assumed. Notice the evolution's sensitivity to the offset irradiation conditions, as well as the marked ω_r modulation observed under MAS. For $I_z = |-1\rangle$, the nutation behavior can be simply derived from $\rho_{-1,-1}(\tau) = -\rho_{1,1}(\tau)$.

varying the overtone irradiation frequency (or of accounting for a chemical shift) via the offset term $\Delta = 2\omega_0^I - \omega_{irr}$.

Equation 6 is a 2×2 Hamiltonian with time-independent coefficients, and hence it enables an analytical calculation of the populations' behavior upon rf irradiation as a function of the nutation time τ. This can in turn be used to infer basic characteristics of a heteronuclear $I-S$ recoupling experiment, whose dipolar evolution will eventually be dictated by the time dependence of the I_z eigenstates. The left-hand column in Figure 1 presents the time evolution of the $|+1\rangle$ populations that can be expected from this static Hamiltonian, calculated for typical quadrupole and rf coupling parameters over a powdered sample and as a function of the offset employed in the overtone irradiation. It becomes evident from these powder averages that small perturbations will be imparted on I_z except for a relatively narrow range of irradiation offsets, and that for this appropriate offset range considerable orientation-dependent oscillations in the $|\pm1\rangle$ states will occur within a time scale of $0.1-1$ ms. Both of these features can be understood from the fact that the overtone irradiation Hamiltonian is composed of a relatively large longitudinal component ($\sim 10^5$ Hz) stemming from the sizable second-order quadrupole effects $\omega_q^{(2)}$, plus a smaller transverse component ($\sim 10^3$ Hz) proportional to $\epsilon\omega_1$. Thus, only when the former is compensated by suitable irradiation offsets Δ will substantial deviations from equilibrium occur, with oscillations in the 10^{-3} s time scale.

Describing the nature of overtone experiments becomes more challenging upon introducing sample spinning. The nutation Hamiltonian is still composed in this case by a 2×2 matrix, but since it is not self-commuting and its coefficients are now time-dependent, it does not permit an analytical calculation of the spins' evolution. The $I = 1$ dynamics under the action of overtone irradiation can still be calculated albeit numerically, via the time-ordered propagation of the spins' density matrix. Assuming an initial $\rho_0 = I_z$ state, this time evolution will be given by $\rho(\tau) = U^\dagger \rho_0 U$, where $U = T \exp\{-i\int_0^\tau H_{nutation}(t')\, dt'\}$ is the propagation operator. The time dependence of the f and g functions involved in $\omega_q^{(2)}$ and $H_{nutation}$ can in turn be derived with the aid of Wigner rotation matrixes, which we define in this case according to the time-dependent Euler transformations

$$\mathrm{PAS}(Q) \xrightarrow{\Omega_2 = \{\alpha,\beta,\gamma\}} \mathrm{ROTOR} \xrightarrow{\Omega_1 = \{\omega_r t, \theta = 54.7°, 0°\}} \mathrm{LAB} \quad (7)$$

where a collinear sample spinning/rf coil setup fixed at the magic angle was assumed. The explicit forms taken by the $f(t)$, $g(t)$ functions following these transformations are given as Supporting Information.

With the aid of these functions, the relevant Hamiltonian can be written and its effects propagated as a function of the nutation pulse length. The right-hand side of Figure 1 shows the time evolution that can then be calculated for the $|+1\rangle$ spin eigenstate of I as a function of the overtone MAS irradiation. Comparable in both static and spinning cases are the offset-dependencies exhibited by the nutation, which only show substantial departures from the equilibrium when $\Delta \approx -\omega_q^{(2)}$. This is because the MAS rates being considered here are approximately an order of magnitude smaller than the average $|\omega_q^{(2)}|$, and therefore fail to introduce substantial modulations into these longitudinal couplings. Different, however, are the actual nutation profiles exhibited by static and MAS cases for the range $\Delta \approx -\omega_q^{(2)}$ of maximum spin excitation. For static cases, the nutation behavior is made up of a complex superposition of frequencies, whereas in the spinning case a well-defined ω_r modulation of the nutation emerges over the complete powder. This feature has important consequences for enhancing the efficiency of dipolar MAS recoupling, and its origin can be gathered from examining the matrix elements in eq 6. On compensating $\omega_q^{(2)}$ with a suitable irradiation offset, this nutation Hamiltonian ends up exhibiting mainly transverse components proportional to $\omega_1\epsilon f$, $\omega_1\epsilon g$. In the static case f, g adopt different values depending on a crystallite's orientation, and the powder-averaged nutation plots thus display interfering $\{\cos(\omega_1\epsilon f\tau), \cos(\omega_1\epsilon g\tau)\}$ oscillations. When undergoing MAS, however, the f and g functions themselves acquire $\{\pm\omega_r, \pm 2\omega_r\}$ time dependencies. The resulting overtone spin nutation curves are then composed of terms of the type $\{\cos[\omega_1\epsilon|f|\cos(n\omega_r t)], \cos[\omega_1\epsilon|g|\cos(n\omega_r t)]\}$, representing Bessel series of base ω_r. In terms of their frequency spectra, these nutations will thus resemble sideband-like structures that contain substantial components oscillating at ω_r regardless of the magnitudes of $|f|$, $|g|$, i.e., regardless of a crystallite's orientation. Hence, the basic ω_r modulation and relatively high coherence are displayed by the MAS overtone nutation plots, even after considering their powder integration.

2.2. Overtone Rotary Recoupling of Heteronuclear Interactions. The significant frequency components that the MAS-driven overtone nutation $|\pm1\rangle$ of populations display in the neighborhood of ω_r will enable the efficient recoupling of $^{14}N-S$ dipolar couplings even under fast MAS. Indeed, these I_z nutations will alter the evolution of the $S-{}^{14}N$ coupled pairs, preventing the MAS refocusing of their mutual dipolar couplings at the end of each rotor echo. The dephasing that will then affect the S-spin signal will depend on a variety of factors including the dipolar coupling, the spinning rate, the offset of overtone irradiation, and the magnitude of the overtone nutation rate $\epsilon\omega_1$.

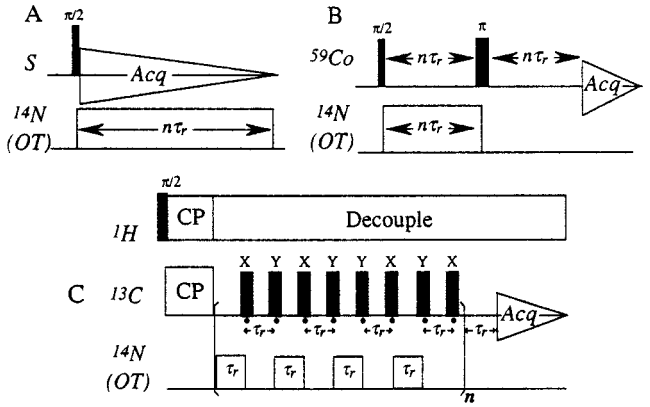

Figure 2. Different ORR pulse sequences considered throughout this study. (A) Basic overtone (OT) version used for understanding the sequence's behavior. (B) Single spin−echo variant, used during actual observations involving ^{59}Co (a spin-$^7/_2$ nucleus). (C) Multiple spin−echo variant incorporating an XY-type phase cycling and complete refocusing of isotropic and anisotropic chemical shifts, employed for the ^{13}C measurements. In the actual experiments the *S*-spin−echo signals were measured with (S) and without (S_0) ^{14}N overtone rf irradiation, to quantify the dephasing fraction $\Delta S/S_0$.

The present section explores these dependencies, assuming for the sake of simplicity the application of the sequence in Figure 2A on an *S*-site devoid of any internal couplings (even if for actual experiments, spin−echo variants such as those shown in Figure 2B,C need to be used to cancel out internal *S*-spin shift interactions).

A quantitative analysis of the overtone rotary recoupling process builds on the effective spin-$^1/_2$ formalism of the previous paragraph but expands it to a coupled $I-S$ space capable of accounting for the two-spin dipolar interaction. Assuming $S = {}^1/_2$ (or the central transition of a half-integer quadrupole nucleus *S*), the resulting 4 × 4 Hamiltonian then reads

$$H_{\mathrm{ORR}}(t) = H_{\mathrm{nutation}}(t) + H_{\mathrm{IS}}(t) =$$

$$\begin{bmatrix} \Delta^I + \omega_q^{(2)} + \frac{1}{2}\omega_{IS}^D(t) & \frac{\omega_1\epsilon}{\sqrt{3}}(\sqrt{2}f(t) + g(t)) & 0 & 0 \\ \frac{\omega_1\epsilon}{\sqrt{3}}(\sqrt{2}f^*(t) + g^*(t)) & -\Delta^I - \omega_q^{(2)} - \frac{1}{2}\omega_{IS}^D(t) & 0 & 0 \\ 0 & 0 & \Delta^I + \omega_q^{(2)} - \frac{1}{2}\omega_{IS}^D(t) & \frac{\omega_1\epsilon}{\sqrt{3}}(\sqrt{2}f(t) + g(t)) \\ 0 & 0 & \frac{\omega_1\epsilon}{\sqrt{3}}(\sqrt{2}f^*(t) + g^*(t)) & -\Delta^I - \omega_q^{(2)} + \frac{1}{2}\omega_{IS}^D(t) \end{bmatrix} \quad (8)$$

Here, all definitions regarding the ^{14}N derive from eq 6 under MAS conditions. The time-dependent dipolar term $\omega_{IS}^D(t)$ that now also needs to be considered can be evaluated using a coordinate transformation similar to that employed for the quadrupolar terms:

$$\mathrm{PAS}(D) \xrightarrow{\Omega_3=\{\varphi=0°,\xi,\psi\}} \mathrm{PAS}(Q) \xrightarrow{\Omega_2=\{\alpha,\beta,\gamma\}} \mathrm{ROTOR} \xrightarrow{\Omega_1=\{\omega_r t,\theta=54.7°,0°\}} \mathrm{LAB} \quad (9)$$

where the Euler angle set Ω_3 transforms the dipolar tensor from its principal axis system (PAS) along the internuclear $I-S$ vector, into *I*'s quadrupolar PAS. The dipolar anisotropy is then related to the r_{IS} internuclear distance by the successive Wigner rotations

$$\omega_{IS}^D(t) = \frac{-2\hbar\gamma_I\gamma_S}{r_{IS}^3}\sqrt{\frac{2}{3}}\sum_{m=-2}^{2}\sum_{n=-2}^{2} D_{m,0}^2(\Omega_1)D_{n,m}^2(\Omega_2)D_{0,n}^2(\Omega_3) \quad (10)$$

The explicit expressions then resulting for $f(t)$, $g(t)$, and $\omega_{IS}^D(t)$ are given as Supporting Information.

Calculating the effective time propagator $U(\tau)$ arising from eq 8 again requires a time-ordered series of numerical diagonalizations and multiplications of H_{ORR}. From this operator the *S*-spin NMR signal can be derived as

$$S(\tau) = \mathrm{Tr}[\rho(\tau)S_+] = Tr[U^\dagger(\tau)S_xU(\tau)S_+] \quad (11)$$

where S_x is assumed as the initial spin state and $S_+ = S_x + iS_y$ is the single quantum coherence being detected. As in most double-resonance experiments, it is customary to compare this signal with S_0, the expectation in the absence of any *I* irradiation, and from here to calculate a dephasing fraction $(S_0 - S)/S_0 = \Delta S/S_0$. For the type of experiment being considered here, this fraction will follow from the powder average

$$\frac{\Delta S}{S_0}(\tau) = \frac{2}{3}\left(1 - \frac{1}{4\pi}\int_0^{2\pi}\int_0^{\pi}\int_0^{2\pi}\mathrm{Tr}\{\rho(\tau)S_+\}\,\mathrm{d}\alpha\,\sin\beta\,\mathrm{d}\beta\,\mathrm{d}\gamma\right) \quad (12)$$

The $^2/_3$ factor in this equation accounts for the fact that in overtone ^{14}N NMR, the $|0\rangle$ eigenstate remains unchanged and hence does not contribute to the *S*-spin dephasing.

Figure 3 presents $\Delta S/S_0$ curves computed under these assumptions for typical sets of coupling values upon systematically changing the $I-S$ dipolar coupling (A), the offset of overtone irradiation (B), the relative orientation between the *I* quadrupolar and $I-S$ dipolar tensors (C), the sample spinning rate (D), and the strength of overtone irradiation (E). These curves evidence maximum dephasing fractions $\Delta S/S_0 \approx 0.67$ developing within $\{\gamma_I\gamma_S/r_{IS}^3\}^{-1}$ time scales, confirming the competitiveness of this form of recoupling. It is also clear that not only the magnitude but, to a lesser extent, also the relative orientation between dipolar and quadrupolar tensors will influence the decay. The conditions for optimal dephasing also vary slightly upon changing the combination of spinning and rf nutation frequencies, with stronger ω_1 fields favoring dephasing at slightly larger ω_r rates. Because of the MAS-modulated nature of the overtone nutation, however, any given ω_r rate will result in an efficient dephasing over a range of applied rf field strengths: no special rotary resonance conditions have to be met for performing this kind of experiment.

One of the most interesting applications of overtone recoupling derives from the selectivity that the heteronuclear dephasing displays to the offset of *I* rf irradiation. To illustrate this potential, Figure 4 focuses on directly bonded model ^{13}C−^{14}N spin pairs and shows the dephasing fractions that for a fixed period of dephasing can be expected from the ^{13}C as a function of the ^{14}N overtone irradiation offset. The close relation between the overtone recoupling offset dependence and ideal second-order quadrupole line shapes is evidenced by these simulations. It is also illustrative to contrast this behavior with the expectations arising from the conventional recoupling of ^{14}N, based on irradiation fields centered at ω_0^I.[17,18] Toward this end, Figure 5 presents, again for model ^{13}C−^{14}N pairs, the dephasing profiles that can be expected from constant-time ORR and TRAPDOR experiments as a function of the ^{14}N irradiation offset. These plots evidence the resemblance that the $\Delta S/S_0$ fractions of these two techniques have to second- and first-order

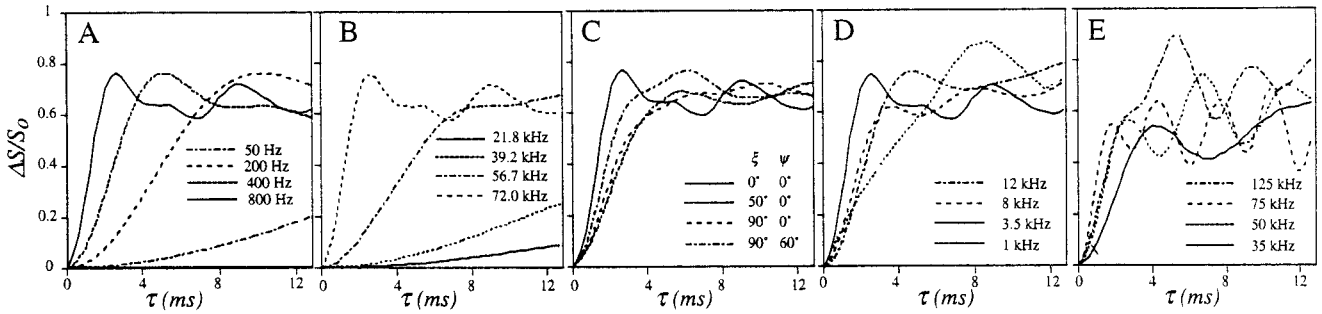

Figure 3. $\Delta S/S_0$ overtone dipolar-dephasing fractions predicted for typical $^{13}C-^{14}N$ sets of coupled spins upon systematically changing the $I-S$ dipolar coupling (A), the offset of overtone irradiation (B), the relative orientation between I's quadrupolar and the $I-S$ dipolar tensors (C), the sample spinning rate (D), and the strength of overtone irradiation (E). Unless specifically mentioned, the parameters incorporated in these simulations are $\chi_Q/2\pi = 0.75$ MHz, $\eta_Q = 0$, dipolar coupling = 0.8 kHz, $\omega_r/2\pi = 3.5$ kHz, $\omega_1/2\pi = 60$ kHz, $\xi = \psi = 0°$, overtone irradiation offset = 72 kHz. 20^3 crystallite orientations together with 1.8 μs time increments were assumed for these calculations.

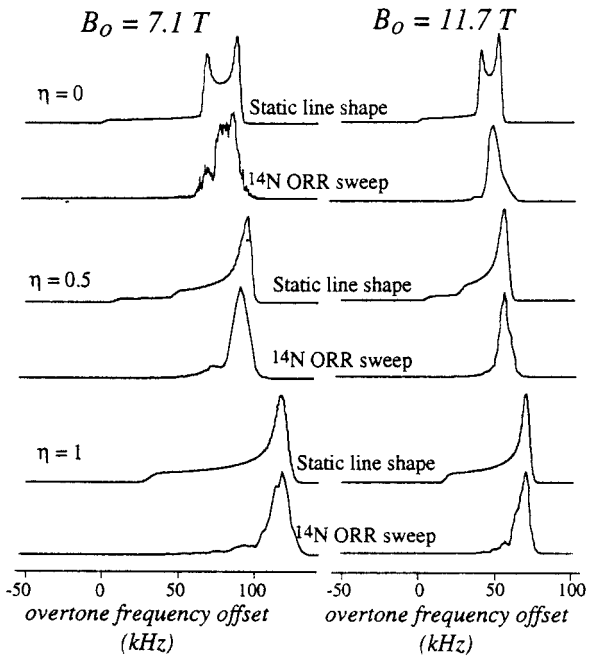

Figure 4. Comparisons between the ideal ^{14}N powder line shapes expected from static overtone experiments, and the S-spin dipolar dephasing fractions expected under MAS conditions as a function of the ^{14}N overtone irradiation offset. Parameters involved: $\chi_Q/2\pi = 0.8$ MHz, $\omega_r/2\pi = 5$ kHz, $S-^{14}N$ dipolar coupling = 0.8 kHz, $\omega_1/2\pi = 37$ kHz, an overtone pulse width fixed at $\tau = 16$ rotor periods, the indicated B_0 field strengths, and various η_Q asymmetry parameter values.

^{14}N quadrupole patterns, respectively. When comparing the relative performance of both techniques in terms of their relative dephasing fractions, it appears that suitably tuned TRAPDOR sequences perform better than their ORR counterparts for weak quadrupoles ($\epsilon \leq 0.1$), while the opposite is the case when ϵ is large.

3. Experimental Details

To test the validity of the various features derived in the preceding paragraph, a series of double ($^{59}Co/^{14}N$)- and triple ($^{1}H/^{13}C/^{14}N$)-resonance experiments were carried out. All samples were analyzed at natural isotopic abundance. These included $^{13}C-^{14}N$ pairs in amino acids and dipeptides: L-alanine (Ala), *N*-acetyl-L-valine (NAV), β-L-alanyl-L-valine (AlaVal), and β-L-aspartyl-L-alanine (AspAla). Also analyzed were the $^{59}Co-^{14}N$ complexes hexaaminecobalt(III) chloride and sodium hexanitrocobaltate(III). ^{13}C signals in the organic samples were acquired under TPPM ^{1}H-decoupling conditions and using an

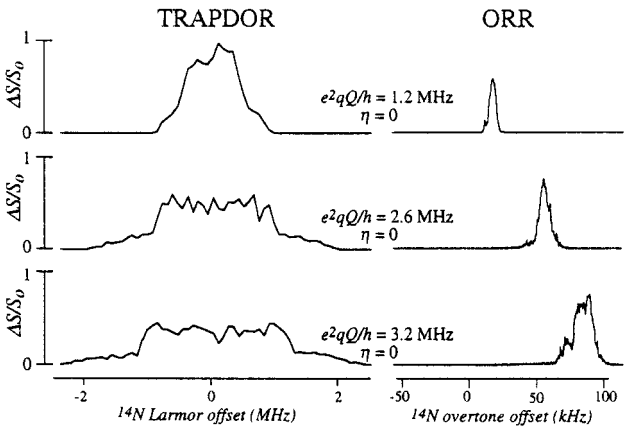

Figure 5. Comparisons between the limiting dipolar $\Delta S/S_0$ fractions resulting as a function of the ^{14}N rf offset when irradiating at the Larmor (TRAPDOR) and at twice the Larmor (ORR) frequency. Calculations assumed a sequence like the one in Figure 2A for both cases; quadrupole coupling parameters were as indicated, B_0 was set at 4.7 T, and all other coupling parameters were as in Figure 4.

XY8-cycled pulse sequence (Figure 2C),[30,31] whereas the single spin–echo version in Figure 2B yielded better sensitivity and fewer distortions when observing the $S = {}^7/_2$ ^{59}Co nucleus. All solid-state NMR spectra were collected on a laboratory-built triple-tuned 7.2-T NMR spectrometer, operating at Larmor frequencies of 301.63, 75.85, and 71.23 MHz for ^{1}H, ^{13}C, and ^{59}Co, respectively; $2 \times 21.80 \approx 43.60$ MHz was the ^{14}N overtone frequency. A 4-mm triple-tuned Varian/Chemagnetics probe and MAS speed controller were used in all experiments, with extensive cooling air applied to prevent potential sample heating during the relatively long periods of ^{14}N overtone irradiation. Powers of 100, 110, and 75 W were applied on the ^{1}H, $^{13}C/^{59}Co$, and ^{14}N overtone rf channels, which delivered 75, 50, and 33 kHz rf fields, respectively (the last of these field calibrated using the nearby ^{2}H resonance of $^{2}H_2O$ at 46.4 MHz). Acquisition scans were alternated between sequences with and without ^{14}N irradiation periods in order to collect S and S_0 signals simultaneously; further experimental details are given underneath each figure's caption.

4. Results

As an example of the feasibility of carrying out ORR-based experiments, Figure 6 illustrates the dephasings exhibited by a series of ^{13}C and ^{59}Co sites proximate to ^{14}N's which are undergoing overtone irradiation. Although ^{13}C's are directly bonded to nitrogens, some of the ^{13}C resonances do not exhibit,

(30) Gullion, T.; Baker, D. B.; Conradi, M. S. *J. Magn. Reson.* **1990**, *89*, 479.
(31) Bennett, A. E.; Rienstra, C. M.; Auger, M.; Lakshmi, K. V.; Griffin, R. G. *J. Chem. Phys.* **1995**, *103*, 6951.

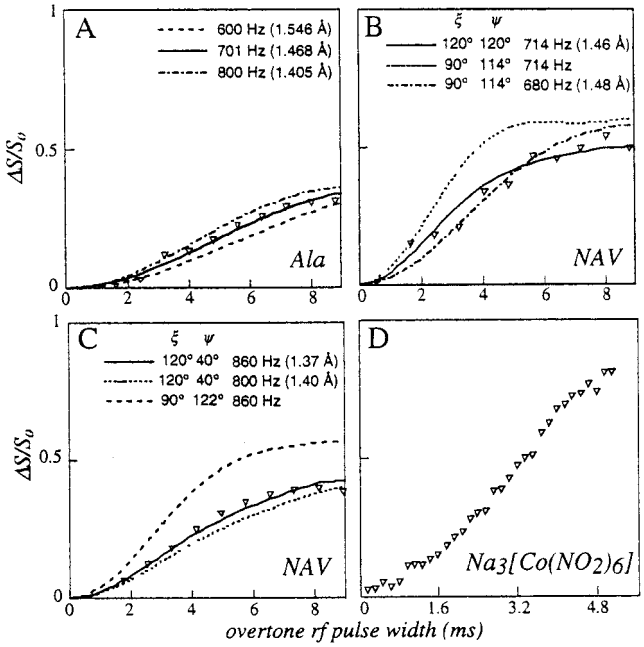

Figure 6. Experimental (symbols) vs calculated (lines) ORR dephasing curves observed for the $C_\alpha-{}^{14}N$ pair of L-alanine (A), for $C_\alpha-{}^{14}N$ (B) and $OC-{}^{14}N$ (C) sites in NAV, and for $^{59}Co-{}^{14}N$ in sodium hexanitrocobaltate(III) (D). Rf overtone fields were in all cases set at 33 kHz. The pulse sequence in Figure 2C ($\omega_r/2\pi = 5$ kHz) was used for the organic samples, whereas the sequence in Figure 2B ($\omega_r/2\pi = 6.25$ kHz) was applied for the inorganic complex. The best fit for L-alanine $C_\alpha-N$ dephasing data matches the literature parameters: $r_{N-C} = 1.468$ Å and coinciding dipolar, quadrupolar tensors.[16] The $C_\alpha-N$ and $OC-N$ data of NAV were fitted with dipolar couplings of 714 Hz ($r_{N-C} = 1.468$ Å) with $\xi \approx 120°$, $\psi \approx 120°$, and 864 Hz ($r_{N-C} = 1.369$ Å) with $\xi \approx 120°$, $\psi \approx 40°$. The optimal offset irradiation position for each of these samples was determined from ^{14}N overtone experiments such as those depicted in Figure 8.

even under optimized conditions, the full dephasing fraction of 0.67; this is a combination of having employed too weak rf fields and of the sites' relatively small quadrupole couplings. In all cases, however, the experimental behavior exhibits a good match when compared to numerical expectations arising from the treatment of the preceding section. For the ^{59}Co sample, the ORR-driven dephasing actually exceeds the 0.67 fraction, despite involving longer $^{59}Co-{}^{14}N$ distances, a behavior that we ascribe to the presence of six nitrogens in the metal's vicinity.

Quantitative dephasing data could also be collected for ^{13}C sites that were not directly bonded to ^{14}N. Figure 7, for instance, shows the ORR curves observed for two terminal carboxyl carbons of β-AspAla, whose dephasing rates are in good agreement with the 3.63 Å (47 Hz coupling) and 2.38 Å (164 Hz coupling) distances observed by crystallography to their nearest ^{14}N.[34] An interesting feature demonstrated by these curves, as well as by some of the curves in Figure 6, is the dephasing's sensitivity on the dihedral angle between the ^{14}N quadrupolar PAS and the $C-N$ internuclear vector. This suggests potential applications to orienting the former within the molecular frame or, if the quadrupole tensor orientation is known, to constrain molecular geometries in the solid phase.

The various dephasing experiments summarized in Figures 6 and 7 were obtained after defining suitable overtone irradiation offsets. This procedure, in turn, involved selecting a sufficiently long dephasing time τ, usually fixed between 12 and 16 rotor cycles, and then monitoring the $\Delta S/S_0$ fraction while sweeping the overtone rf irradiation frequency. After the ^{13}C or ^{59}Co NMR

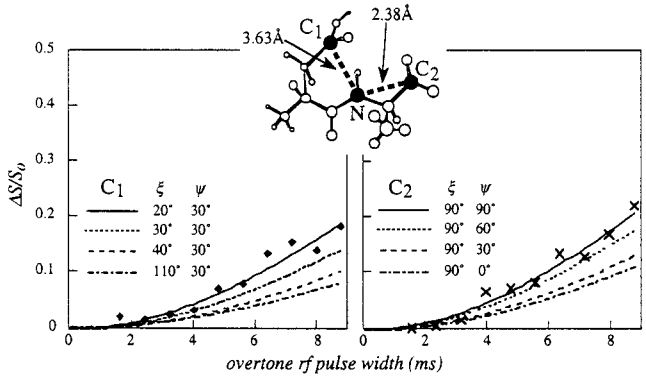

Figure 7. Same as in Figure 6, but involving $^{13}C-{}^{14}N$ dipolar couplings between pairs of peptide nitrogen and carbonyl carbons separated by more than one bond. In this β-AspAla structure (top), the amide nitrogen is separated by four bonds from the side-chain carbon C_1 (3.63 Å) and by two bonds from carbon C_2 (2.38 Å).[34] The $-NH_3^+$ nitrogen in the structure has a very different offset for its overtone excitation and could thus be ignored when analyzing dephasing processes that involve irradiation of the amide ^{14}N.

signals were Fourier transformed as a fraction of their acquisition times, these experiments resulted in what effectively amounts to a two-dimensional plot, correlating the isotropic *S* MAS traces with the overtone spectra of their nearby nitrogen sites (Figure 8). This offset dependence, the origin of which was alluded to earlier (Figures 4 and 5), endows the method with a selective chemical specificity that is not usually available in dipolar recoupling methods. This allowed us, for instance, to analyze the ^{13}C dephasing in the AlaVal and AspAla dipeptides (Figure 7) solely on the basis of distances to amide nitrogens; $-NH_3^+$ groups, having smaller quadrupolar couplings, undergo ORR at significantly different irradiation offsets and thus can be considered in this recoupling analysis as if they were isotopically different species.

Besides their usefulness in setting up site-specific recoupling experiments, variable-offset/fixed-evolution time ORR experiments provide a route to acquiring high-resolution overtone spectra from spinning powders that, at least in our experience, is considerably simpler and more sensitive than comparable direct-detection ^{14}N overtone schemes. The meaningful overtone spectral data arising from these indirect dephasing signals can be better appreciated in Figure 9, which compares the offset dependence of several experimental ORR line shapes with the ideal overtone powders expected from ^{14}N literature quadrupole couplings. The line shape agreement is very good when dealing with an isolated $^{13}C-{}^{14}N$ pair. Even when dealing with numerous coupled nitrogens such as in the cobalt(III) complexes, these experiments enable reasonable estimates for the hitherto unavailable ^{14}N coupling constants.

5. Discussion and Conclusions

The present study demonstrates that overtone experiments involving forbidden $|+1\rangle \leftrightarrow |-1\rangle$ ^{14}N transitions can act as suitable and efficient means for dipolar recoupling under MAS. To analyze the behavior observed during these experiments and quantify their dephasing performance, a simple formalism was derived, based on an effective spin-$^1/_2$ Hamiltonian describing overtone nutation. From here the offset dependence and high recoupling efficiency of the method could be rationalized, the

(32) Lucken, E. A. C. *Nuclear Quadurople Coupling Constants*; Academic Press: London, 1963.
(33) Terao, T. *J. Mol. Struct.* **1998**, *441*, 283.
(34) Gorbitz, C. H. *Acta Chem. Scand.* **1987**, *B41*, 679.

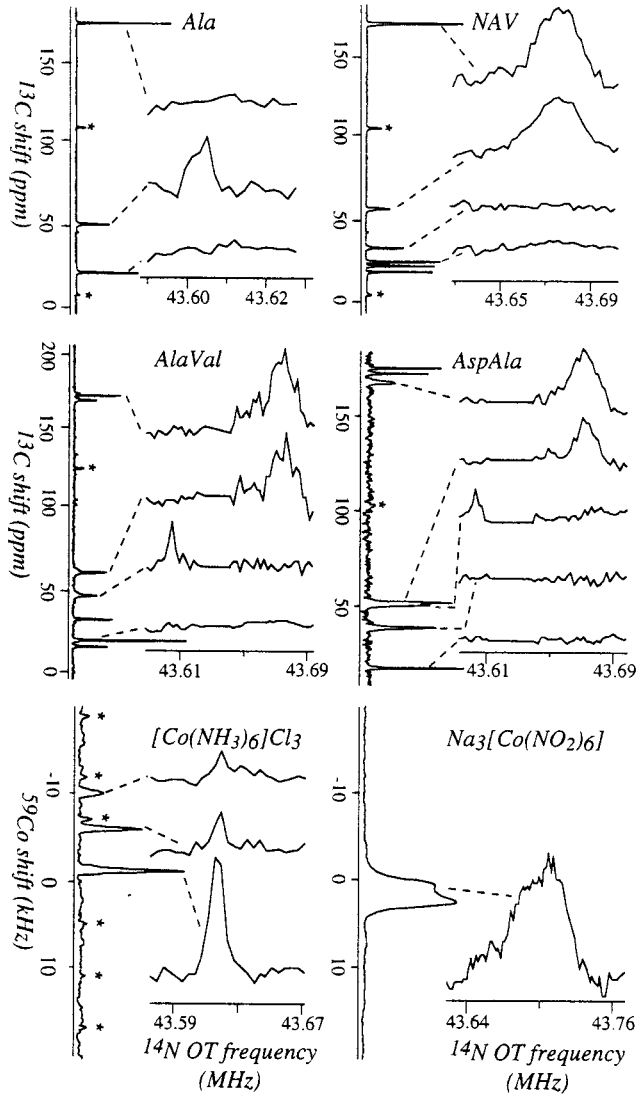

Figure 8. ^{14}N overtone powder line shapes detected for the indicated sample sites, as deduced from the $\Delta S/S_0$ dephasing fractions observed from ^{13}C CPMAS and ^{59}Co MAS NMR spectra. The overtone dimensions were swept in 2 kHz steps. The spinning speed was 5 kHz in all measurements, and asterisks denote spinning sidebands. Between 32 and 512 scans were collected for both S and S_0 measurements at each overtone irradiation frequency, depending on the compound.

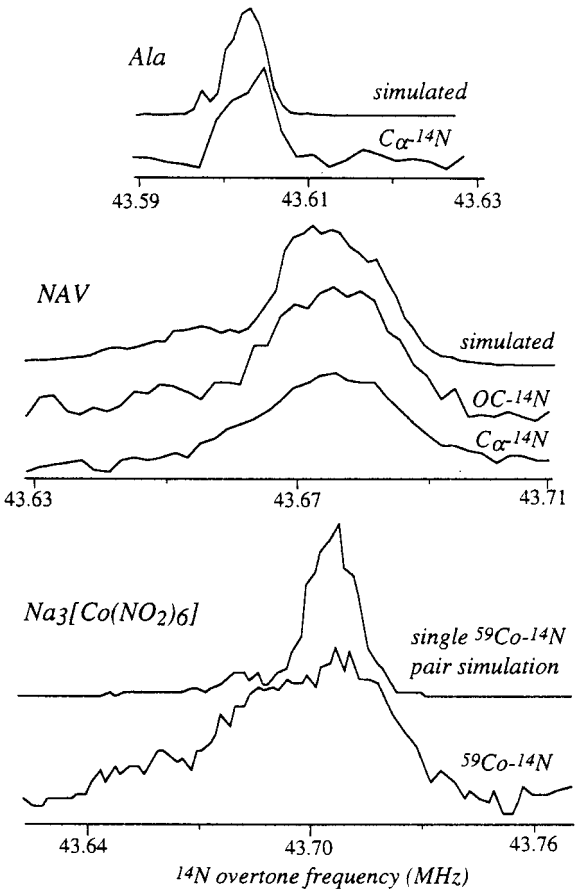

Figure 9. Comparisons between the experimental ^{14}N powder line shapes inferred from the $\Delta S/S_0$ dephasing fractions (Figure 8), and best-fit powder patterns expected from ideal ^{14}N overtone experiments. Simulations incorporate $\chi_Q/2\pi = 0.3$ MHz and $\eta_Q = 0$ for L-alanine,[16] $\chi_Q/2\pi = 0.8$ MHz $\eta_Q = 0.3$ for NAV,[26] and a single ^{59}Co$-^{14}$N pair with $\chi_Q/2\pi = 0.9$ MHz, $\eta_Q = 0.4$ for sodium hexanitrocobaltate(III). All calculations were referred with respect to the exact experimental $2 \times \omega_0^{^{14}N}$ frequency, 43.596 MHz.

former stemming from the large second-order quadrupole effects involved, and the latter from the periodic time dependence imposed by spinning on the transverse irradiation terms $\{\epsilon f, \epsilon g\}$. In some respects the latter aspect of overtone recoupling resembles that of certain spin-$^1/_2$ schemes such as MORE,[13,14,33] which rely on amplitude-modulated rf fields for recoupling the dipolar couplings. These amplitude modulations provide a MAS dipolar recoupling scheme which is remarkably efficient and independent of rf inhomogenities. A difference between the two classes of sequences is that, whereas in the spin-$^1/_2$ experiments ω_r modulations need to be artificially introduced on the amplitude ω_1, in the ORR case they are natural consequences of the modulations imposed by MAS on the overtone nutation Hamiltonian.

Among the basic features found for this new form of recoupling are a conventional dependence on the $I-S$ dipolar coupling, weak yet non-monotonic dependencies on the rf field strength and spinning rates used in the recoupling, a sensitivity with regard to the relative orientations of the tensors involved, and considerable efficiency losses as the $\epsilon = \chi_Q/\omega_0^I$ ratio drops below $\approx$0.05. Also worth noting is the narrow-band nature of the recoupling, which allows one to discriminate the dephasing according to the quadrupole parameters of the coupled ^{14}N site. Further clarification on the influences of these factors would clearly benefit from a simpler model, capable of describing ORR phenomena and their resulting dephasing curves in analytical terms. Additional theoretical and experimental work is also needed to clarify whether the combined dependence of the ORR dephasing on multiple coupling parameters, particularly on the quadrupolar coupling parameters of the irradiated nucleus, ends up being an asset or a liability for geometrical assessments. Efforts along all these research lines are actively under way, yet it is satisfactory to note that even at this stage, experimental data show a very good agreement with the numerical predictions derived from our numerical formalism.

In addition to its structure measurement potential, one of the most promising aspects of this technique is its ability to report overtone spectra via sweeps of the irradiation recoupling field. This information arises in a fashion that is largely independent of the specific recoupling conditions, which therefore do not need to be precisely known or set, and provides reliable line shapes from the elusive realm of strongly coupled quadrupolar NMR. Given the relevance of ^{14}N in a variety of synthetic and biological structures and the well-characterized correlations

relating its quadrupole parameters with surrounding electronic density,[32] this may result in a most valuable ramification of the present technique. Also intriguing is the possibility of extending this high-resolution spectroscopic approach to other strongly coupled species with spin numbers $I \geq {}^3/_2$. Indeed, a number of half-integer quadrupoles (e.g., halogens, ^{63}Cu, etc.) can only be observed by NMR if positioned in highly symmetric environments. We are currently exploring whether overtone recoupling might help to extend this window of observation to more generic sites.

Acknowledgment. This work was supported by the U.S. National Science Foundation through Grants DMR-9806810 and CHE-9841790 (Creativity Extension Award), by the U.S. Department of Energy through Grant 00ER15049, as well as by a Philip M. Klutznick Fund for Research (Weizmann Institute). L.F. is a Camille Dreyfus Teacher-Scholar (1996−2001).

Supporting Information Available: Explicit expressions for the various functions involved in eq 8 and needed to derive the ORR dephasing curves (PDF). This material is available free of charge via the Internet at http://pubs.acs.org.

JA0113798